

Intramolecular Electron Transfer within the Substituted Tetrathiafulvalene–Quinone Dyads: Facilitated by Metal Ion and Photomodulation in the Presence of Spiropyran

Hui Wu,^{†,‡} Deqing Zhang,^{*,†} Lei Su,[†] Kei Ohkubo,[§] Chunxi Zhang,[†] Shiwei Yin,[†] Lanqun Mao,[†] Zhigang Shuai,[†] Shunichi Fukuzumi,[§] and Daoben Zhu^{*,†}

Contribution from the Beijing National Laboratory for Molecular Sciences, Organic Solids Laboratory, Institute of Chemistry, Chinese Academy of Sciences, Beijing 100080, China, Graduate School of Chinese Academy of Sciences, Beijing 100080, China, and Department of Material and Life Science, Division of Advanced Science and Biotechnology, Graduate School of Engineering, Osaka University, SORST, Japan Science and Technology Agency (JST), Suita, Osaka 565-0871, Japan

Received January 14, 2007; E-mail: dqzhang@iccas.ac.cn

Abstract: Intramolecular electron transfer is observed for two new substituted tetrathiafulvalene (TTF)–quinone dyads **1** and **2** in the presence of metal ions. On the basis of the electrochemical studies of reference compound **5** and the comparative studies with dyad **3**, it was proposed that the synergic coordination of the radical anion of quinone and the oligoethylene glycol chain with metal ions may be responsible for stabilizing the charge-separation state and thus facilitating the electron-transfer process. Most interestingly, the intramolecular electron-transfer processes within these two dyads can be modulated by UV–vis light irradiation in the presence of spiropyran, by taking advantage of its unique properties.

1. Introduction

Tetrathiafulvalene (TTF) and its derivatives as strong electron donors have been extensively investigated as the components of organic conductors and superconductors for the past 3 decades.¹ In recent years, electron donor (D)–acceptor (A) molecules with TTF as the electron-donating unit have received significant attention.^{2–11} This is mainly because (1) these D–A molecules show potential photovoltaic applications by taking advantage of efficient photoinduced electron-transfer (PET) processes between TTF and electron-accepting units (e.g., C₆₀); (2) these D–A molecules can be employed as models to study charge-transfer (CT) interactions. The electron-accepting units which have been covalently linked to TTF units include quinone,⁴ C₆₀,⁵ TCNQ (tetracyano-*p*-quinodimethane),^{6,7} perylene

diimide,⁸ naphthalene diimide,⁹ and porphyrin/phthalocyanine,¹⁰ etc. We have recently described redox molecular fluorescence switches and chemical sensors based on TTF–anthracene dyads.¹¹

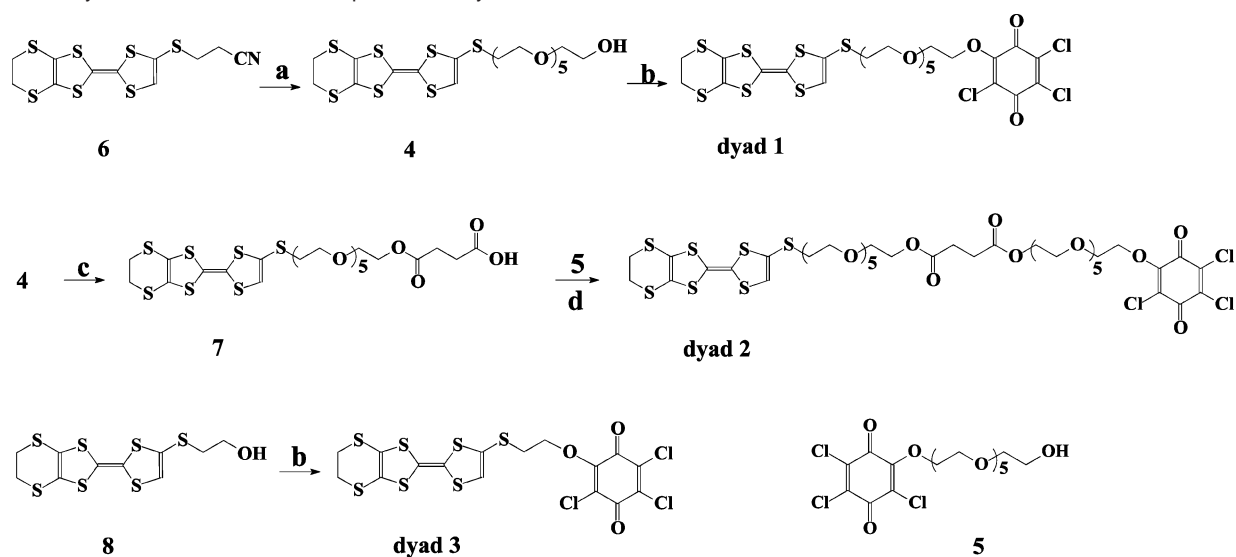
In comparison to the intramolecular photoinduced electron transfer, the intramolecular electron transfer has seldom been observed for D–A molecules containing TTF units. Perepichka et al. and later Tsiperman et al. have very recently described

[†] Institute of Chemistry, Chinese Academy of Sciences.

[‡] Graduate School of Chinese Academy of Sciences.

[§] Osaka University.

- (1) (a) Williams, J. M.; Ferraro, J. R.; Thorn, R. J.; Carlson, K. D.; Geiser, U.; Wang, H. H.; Kini, A. M.; Whangbo, M.-H. *Organic Superconductors (Including Fullerenes)*; Prentice Hall: Englewood Cliffs, NJ, 1992. (b) Coronado, E.; Day, P. *Chem. Rev.* **2004**, *104*, 5419–5448. (c) Shibaeva, R. P.; Yagubskii, E. B. *Chem. Rev.* **2004**, *104*, 5347–5378. (d) Yamada, J.-i.; Akutsu, H.; Nishikawa, H.; Kikuchi, K. *Chem. Rev.* **2004**, *104*, 5057–5084.
- (2) (a) Bryce, M. R. *Adv. Mater.* **1999**, *11*, 11–23. (b) Bryce, M. R. *J. Mater. Chem.* **2000**, *10*, 589–598. (c) Segura, J. L.; Martín, N. *Angew. Chem., Int. Ed.* **2001**, *40*, 1372–1409. (d) Bendikov, M.; Wudl, F.; Perepichka, D. F. *Chem. Rev.* **2004**, *104*, 4891–4945.
- (3) (a) Pease, A. R.; Jeppesen, J. O.; Stoddart, J. F.; Luo, Y.; Collier, C. P.; Heath, J. R. *Acc. Chem. Res.* **2001**, *34*, 433–444. (b) Jeppesen, J. O.; Perkins, J.; Becher, J.; Stoddart, J. F. *Angew. Chem., Int. Ed.* **2001**, *40*, 1216–1221. (c) Tseng, H.; Vignon, S.; Stoddart, J. F. *Angew. Chem., Int. Ed.* **2003**, *42*, 1491–1495. (d) Liu, Y.; Flood, A. H.; Stoddart, J. F. *J. Am. Chem. Soc.* **2004**, *126*, 9150–9151. (e) Steuerman, D. W.; Tseng, H.; Peters, A. J.; Flood, A. H.; Jeppesen, J. O.; Nielsen, K. A.; Stoddart, J. F.; Heath, J. R. *Angew. Chem., Int. Ed.* **2004**, *43*, 6486–6491.
- (4) (a) Frenzel, S.; Müllen, K. *Synth. Met.* **1996**, *80*, 175–182. (b) Segura, J. L.; Martín, N.; Seoane, C.; Hanack, M. *Tetrahedron Lett.* **1996**, *37*, 2503–2506. (c) Scheib, S.; Cava, M. P.; Baldwin, J. W.; Metzger, R. M. *J. Org. Chem.* **1998**, *63*, 1198–1204. (d) Moriarty, R. M.; Tao, A.; Gilardi, R.; Song, Z.; Tuladhar, S. M. *Chem. Commun.* **1998**, 157–158. (e) González, M.; Illescas, B.; Martín, N.; Segura, J. L.; Seoane, C.; Hanack, M. *Tetrahedron* **1998**, *54*, 2853–2866. (f) Tsiperman, E.; Regev, T.; Becker, J. Y.; Bernstein, J.; Ellern, A.; Khodorkovsky, V.; Shames, A.; Shapiro, L. *Chem. Commun.* **1999**, 1125–1126. (g) Gautier, N.; Dumur, F.; Lloveras, V.; Vidal-Gancedo, J.; Veciana, J.; Rovira, C.; Hudhomme, P. *Angew. Chem., Int. Ed.* **2003**, *42*, 2765–2768. (h) Dumur, F.; Gautier, N.; Gallego-Planas, N.; Sahin, Y.; Levillain, E.; Mercier, N.; Hudhomme, P.; Masino, M.; Giraldo, A.; Lloveras, V.; Vidal-Gancedo, J.; Veciana, J.; Rovira, C. *J. Org. Chem.* **2004**, *69*, 2164–2177.
- (5) (a) Prato, M.; Maggini, M.; Giacometti, C.; Scorrano, G.; Sandona, G.; Farnia, G. *Tetrahedron* **1996**, *52*, 5221–5234. (b) Martín, N.; Sánchez, L.; Seoane, C.; Andreu, R.; Garín, J.; Orduña, J. *Tetrahedron Lett.* **1996**, *37*, 5979–5982. (c) Llacay, J.; Veciana, J.; Vidal-Gancedo, J.; Bourdeland, J. L.; González-Moreno, R.; Rovira, C. *J. Org. Chem.* **1998**, *63*, 5201–5210. (d) Martín, N.; Sánchez, L.; Illescas, B.; Pérez, I. *Chem. Rev.* **1998**, *98*, 2527–2547. (e) Simonsen, K. B.; Kononov, V. V.; Kononova, T. A.; Kawai, T.; Cava, M. P.; Kispert, L. D.; Metzger, R. M.; Becher, J. *J. Chem. Soc., Perkin Trans. 2* **1999**, 657–665. (f) Guldi, D. M.; González, S.; Martín, N. *J. Org. Chem.* **2000**, *65*, 1978–1983. (g) Martín, N.; Sánchez, L.; Herranz, M. A.; Guldi, D. M. *J. Phys. Chem. A* **2000**, *104*, 4648–4657. (h) Kreher, D.; Cariou, M.; Liu, S.-G.; Levillain, E.; Veciana, J.; Rovira, C.; Gorgues, A.; Hudhomme, P. *J. Mater. Chem.* **2002**, *12*, 2137–2159. (i) Diaz, M. C.; Herranz, M. A.; Illescas, B. M.; Martín, N.; Godbert, N.; Bryce, M. R.; Luo, C.; Swartz, A.; Anderson, G.; Guldi, D. M. *J. Org. Chem.* **2003**, *68*, 7711–7721. (j) Gorgues, A.; Hudhomme, P.; Sallé, M. *Chem. Rev.* **2004**, *104*, 5151–5184. (k) Baffreau, J.; Dumur, F.; Hudhomme, P. *Org. Lett.* **2006**, *8*, 1307–1310.

Scheme 1. Synthetic Scheme for the Preparation of Dyads 1–3^a

^a Reagents and conditions: (a) CsOH·H₂O, hexaethyleneglycol–monotoluenesulfonate, THF, ambient temperature; (b) NaH, tetrachloro-1,4-benzoquinone, THF, ambient temperature; (c) succinic anhydride, K₂CO₃, DMF, ambient temperature; (d) DCC, DMAP, CH₂Cl₂, ambient temperature.

the charge/electron transfer within the TTF–TCNQ dyads.⁷ Only in one substituted TTF–quinone dyad with a short rigid spacer a weak CT band was observed.^{4f} Herein we report two new substituted TTF–quinone dyads **1** and **2**, each of which has a long oligoethylene glycol chain as the spacer (Scheme 1). The initial motivation of this research is to study the intramolecular donor–acceptor interaction effected by the coordination of the oligoethylene glycol chain with metal ions.¹² It is interesting to note that intramolecular electron transfer is indeed observed for dyads **1** and **2** in the presence of metal ion (Pb²⁺, Zn²⁺, and Sc³⁺). In order to understand the metal ion-promoted electron-transfer mechanism, comparative studies with reference compounds **3**–**5** were performed. The results indicate that (1) the reduction potential of reference compound **5** is positively shifted to a large extent in the presence of metal ion

(Pb²⁺, Sc³⁺, Zn²⁺), and thus the electron transfer between TTF and quinone units of dyads **1** and **2** would become thermodynamically feasible; (2) the synergic coordination of the oligoethylene glycol chain and the radical anion of quinone with metal ion would stabilize the charge-separation state and thus further facilitate the electron-transfer process.

On the basis of the fact that the intramolecular electron transfer within dyads **1** and **2** is facilitated by metal ion coordination, it is anticipated that the competitive binding of metal ions by additional ligands would affect the electron-transfer processes. It is known that the open form (merocyanine, MC) of spiropyran (SP) can coordinate with metal ions (MC·Mⁿ⁺), while SP does not show this property. By taking advantage of this unique property of SP, we successfully demonstrate that the intramolecular electron-transfer processes within these two dyads can be modulated by alternating UV–vis light irradiation in the presence of SP.

2. Results and Discussion

2.1. Synthesis. The synthetic approaches to dyads **1** and **2** as well as dyad **3** are shown in Scheme 1. Compound **6** was prepared based on the procedure reported by us previously.¹³ Reaction of compound **6** with hexaethyleneglycol monotoluenesulfonate¹⁴ led to compound **4**. Further reaction of compound **4** with tetrachloro-1,4-benzoquinone in the presence of NaH

- (6) (a) Aviram, A.; Ratner, M. *Chem. Phys. Lett.* **1974**, *29*, 277–283. (b) Perepichka, D. F.; Bryce, M. R.; Batsanov, A. S.; Howard, J. A. K.; Cuello, A. O.; Gray, M.; Rotello, V. M. *J. Org. Chem.* **2001**, *66*, 4517–4524 and references therein.
- (7) (a) Perepichka, D. F.; Bryce, M. R.; Pearson, C.; Petty, M. C.; McInnes, E. J. L.; Zhao, J. P. *Angew. Chem., Int. Ed.* **2003**, *42*, 4636–4639. (b) Tsiperman, E.; Becker, J. Y.; Khodorkovsky, V.; Shames, A.; Shapiro, L. *Angew. Chem., Int. Ed.* **2005**, *44*, 4015–4018.
- (8) (a) Guo, X.; Zhang, D.; Zhang, H.; Fan, Q.; Xu, W.; Ai, X.; Fan, L.; Zhu, D. *Tetrahedron* **2003**, *59*, 4843–4850. (b) Leroy-Lhez, S.; Baffreau, J.; Perrin, L.; Levillain, E.; Allain, M.; Blesa, M.-J.; Hudhomme, P. *J. Org. Chem.* **2005**, *70*, 6313–6320.
- (9) Guo, X.; Gan, Z.; Luo, H.; Araki, Y.; Zhang, D.; Zhu, D.; Ito, O. *J. Phys. Chem. A* **2003**, *107*, 9747–9753.
- (10) (a) Blower, M. A.; Bryce, M. R.; Devonport, W. *Adv. Mater.* **1996**, *8*, 63–65. (b) Wang, C.; Bryce, M. R.; Batsanov, A. S.; Stanley, C. F.; Beeby, A.; Howard, J. A. K. *J. Chem. Soc., Perkin Trans. 2* **1997**, 1671–1678. (c) Becher, J.; Brimert, T.; Jeppesen, J. O.; Pedersen, J. Z.; Zubarev, R.; Bjørnholm, T.; Reitzel, N.; Jensen, T. R.; Kjaer, K.; Levillain, E. *Angew. Chem., Int. Ed.* **2001**, *40*, 2497–2500. (d) Farren, C.; Christensen, C. A.; FitzGerald, S.; Bryce, M. R.; Beeby, A. *J. Org. Chem.* **2002**, *67*, 9130–9139. (e) Li, H.; Jeppesen, J. O.; Levillain, E.; Becher, J. *Chem. Commun.* **2003**, 846–847. (f) Loosli, C.; Jia, C.; Liu, S.-X.; Haas, M.; Dias, M.; Levillain, E.; Neels, A.; Labat, G.; Hauser, A.; Decurtins, S. *J. Org. Chem.* **2005**, *70*, 4988–4992.
- (11) (a) Zhang, G.; Zhang, D.; Guo, X.; Zhu, D. *Org. Lett.* **2004**, *6*, 1209–1212. (b) Li, X.; Zhang, G.; Ma, H.; Zhang, D.; Li, J.; Zhu, D. *J. Am. Chem. Soc.* **2004**, *126*, 11543–11548. (c) Zhang, G.; Li, X.; Ma, H.; Zhang, D.; Li, J.; Zhu, D. *Chem. Commun.* **2004**, 2072–2073. (d) Feng, M.; Guo, X. F.; Lin, X.; He, X. B.; Ji, W.; Du, S. X.; Zhang, D. Q.; Zhu, D. B.; Gao, H. *J. Am. Chem. Soc.* **2005**, *127*, 15338–15339. (e) Lu, H.; Xu, W.; Zhang, D.; Chen, C.; Zhu, D. *Org. Lett.* **2005**, *7*, 4629–4632. (f) Zhang, G.; Zhang, D.; Zhao, X.; Ai, X.; Zhang, J.; Zhu, D. *Chem. Eur. J.* **2006**, *12*, 1067–1073. (g) Zhang, G.; Zhang, D.; Zhou, Y.; Zhu, D. *J. Org. Chem.* **2006**, *71*, 3970–3972.

- (12) (a) Baran, P. S.; Monaco, R. R.; Khan, A. U.; Schuster, D. I.; Wilson, S. R. *J. Am. Chem. Soc.* **1997**, *119*, 8363–8364. (b) Brøndstet Nielsen, M.; Lomholt, C.; Becher, J. *Chem. Soc. Rev.* **2000**, *29*, 153–164. (c) Le Derf, F.; Mazari, M.; Mercier, N.; Levillain, E.; Trippé, G.; Riou, A.; Richomme, P.; Becher, J.; Garin, J.; Orduña, J.; Gallego-Planas, N.; Gorgues, A.; Sallé, M. *Chem. Eur. J.* **2001**, *7*, 447–455. (d) Le Derf, F.; Levillain, E.; Trippé, G.; Gorgues, A.; Sallé, M.; Sebastian, R. M.; Caminade, A. M.; Majoral, J. P. *Angew. Chem., Int. Ed.* **2001**, *40*, 224–227. (e) Trippé, G.; Levillain, E.; Le Derf, F.; Gorgues, A.; Sallé, M.; Jeppesen, J. O.; Nielsen, K.; Becher, J. *Org. Lett.* **2002**, *4*, 2461–2464. (f) Lyskawa, J.; Le Derf, F.; Levillain, E.; Mazari, M.; Sallé, M.; Dubois, L.; Viel, P.; Bureau, C.; Palacin, S. *J. Am. Chem. Soc.* **2004**, *126*, 12194–12195. (g) Delogu, G.; Fabbri, D.; Dettori, M. A.; Sallé, M.; Le Derf, F.; Blesa, M.-J.; Allain, M. *J. Org. Chem.* **2006**, *71*, 9096–9103.
- (13) (a) Jia, C.; Zhang, D.; Guo, X.; Wan, S.; Xu, W.; Zhu, D. *Synthesis* **2002**, 15, 2177–2182. (b) Zou, L.; Shao, X.; Zhang, D.; Wang, Q.; Zhu, D. *Org. Biomol. Chem.* **2003**, *1*, 2157–2159.
- (14) McCairn, M. C.; Tonge, S. R.; Sutherland, A. J. *J. Org. Chem.* **2002**, *67*, 4847–4855.

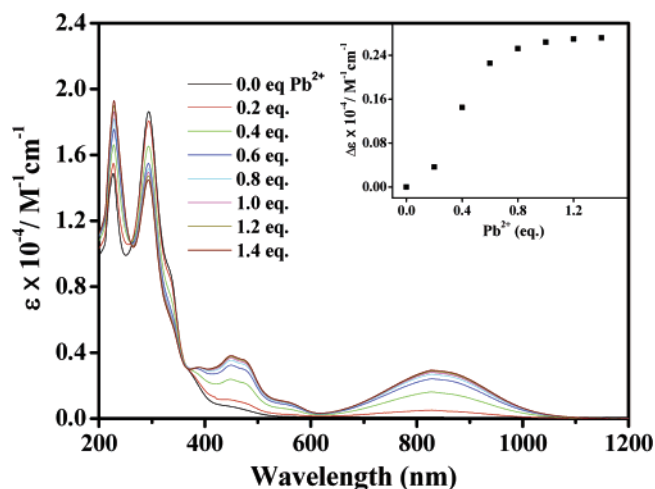


Figure 1. Absorption spectra (with an ϵ scale) of dyad **1** recorded in a mixture of CH_2Cl_2 and CH_3CN (1:1, v/v; 5.0×10^{-5} M) in the presence of increasing amounts of Pb^{2+} [$\text{Pb}(\text{ClO}_4)_2$]; inset shows the variation of ϵ at 845 nm upon addition of 0–1.4 equiv of Pb^{2+} .

afforded dyad **1** in 44% yield after purification (Scheme 1). Compound **4** was allowed to react with succinic anhydride to yield compound **7**, which was then coupled with compound **5** in the presence of DCC/DMAP to yield dyad **2** in 30% yield. Dyad **3** was obtained by the reaction of compound **8**¹³ and tetrachloro-1,4-benzoquinone.

2.2. Absorption and ESR Spectral Studies. Figure 1 shows the absorption spectrum of dyad **1** and those in the presence of different amounts of Pb^{2+} . The absorption spectrum of dyad **1** without addition of Pb^{2+} is almost the superposition of those of the reference compounds **4** and **5**. This result clearly indicates that there is no detectable interaction between the TTF and quinone units of dyad **1** in the absence of Pb^{2+} .

After addition of Pb^{2+} to the solution of dyad **1**, new absorption bands around 450 and 845 nm emerged, and their absorption intensities increased by increasing the amount of Pb^{2+} (Figure 1). According to previous studies,¹⁵ the absorption bands around 450 and 845 nm can be assigned to the radical cation of the TTF unit of dyad **1**. This assumption can also be supported by the spectroelectrochemical studies as discussed below. The same absorption bands at 450 and 845 nm were detected if the solution of dyad **1** was subjected to electrochemical oxidation at 0.80 V (vs Ag/AgCl), higher than the first oxidation potential of the TTF unit of dyad **1**. The inset of Figure 1 shows the variation of the absorbance (with an ϵ scale) at 845 nm vs the molar fraction of Pb^{2+} .¹⁶

As shown in Figure 2, the solution of dyad **1** in the presence of 1.0 equiv of Pb^{2+} exhibited strong doublet ESR signals. The doublet ESR signals were likely due to the radical cation of the TTF unit of dyad **1**, and the doublet signals were ascribed to

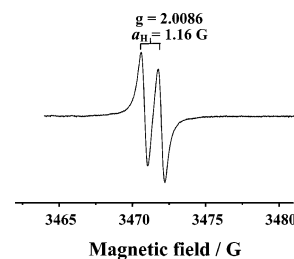


Figure 2. ESR spectrum of dyad **1** (1.0×10^{-4} M) in $\text{CH}_2\text{Cl}_2/\text{CH}_3\text{CN}$ (1:1, v/v) in the presence of 1.0 equiv of Pb^{2+} [$\text{Pb}(\text{ClO}_4)_2$] recorded at room temperature; the solution was degassed before measurement.

the splitting of one H atom of the TTF unit ($g = 2.0086$, $a_{\text{H}} = 1.16$ G). This assumption was supported by the fact that direct oxidation of reference compound **4** by $\text{PhI}(\text{OAc})_2$ and $\text{CF}_3\text{-SO}_3\text{H}$ ^{17a} led to similar doublet ESR signals with $g = 2.0086$ and $a_{\text{H}} = 1.18$ G (see Figure S2 of the Supporting Information). The radical anion was not seen here probably because of the facile disproportionation of the radical anion of quinone ($\text{Q}^{\cdot-}$) into the corresponding Q^{2-} and neutral Q in the presence of metal ion at room temperature.^{16,17b} The possibility of direct oxidation of the TTF unit by Pb^{2+} can be ruled out because a control experiment with reference compound **4** showed that oxidation of **4** by Pb^{2+} did not take place under the same conditions. These results indicated that in the presence of Pb^{2+} intramolecular electron transfer occurred between the TTF and quinone units within dyad **1**,¹⁸ in which the end–end distance between donor and acceptor units was estimated to be 36 Å (see Figure S14 of the Supporting Information).

Among the metal ions tested, Sc^{3+} and Zn^{2+} can also facilitate the intramolecular electron transfer between the TTF and quinone units of dyad **1**. As shown in Figures 3 and 4, absorption bands at 450 and 845 nm due to the TTF radical cation of dyad **1** were detected in the presence of Sc^{3+} and Zn^{2+} .¹⁹ Also, doublet ESR signals were observed (see the insets of Figures 3 and 4).²⁰ These results demonstrated that electron transfer also occurred for dyad **1** in the presence of $\text{Sc}^{3+}/\text{Zn}^{2+}$. When the absorption and ESR spectra of dyad **1** (the same concentration) in the presence of equal amounts of $\text{Sc}^{3+}/\text{Pb}^{2+}/\text{Zn}^{2+}$ are compared, the absorption intensity at 845 nm and ESR signal intensity varied in the following order: $\mathbf{1} + \text{Sc}^{3+} > \mathbf{1} + \text{Pb}^{2+} > \mathbf{1} + \text{Zn}^{2+}$.²¹ This leads us to conclude that Sc^{3+} can promote the electron transfer within dyad **1** more efficiently.

(15) (a) Spanggaard, H.; Prehn, J.; Nielsen, M. B.; Levillain, E.; Allain, M.; Becher, J. *J. Am. Chem. Soc.* **2000**, *122*, 9486–9494. (b) Zhou, Y.; Zhang, D.; Zhu, L.; Shuai, Z.; Zhu, D. *J. Org. Chem.* **2006**, *71*, 2123–2130.

(16) On the basis of the absorbance variation at 845 nm vs the amount of Pb^{2+} , the reaction stoichiometry between dyad **1** (abbreviated as TTF–Q) and Pb^{2+} was estimated to be 2:1. This can be explained as follows: (1) as to be discussed below, addition of Pb^{2+} would lead to the intramolecular electron transfer, and Pb^{2+} is coordinated to the radical anion of the quinone unit and the oligoethylene glycol chain (see Scheme 2), namely, $\text{TTF}^{\cdot+}\text{-Q} + \text{Pb}^{2+} \rightarrow \text{TTF}^{\cdot+}\text{-Q}^{\cdot-}\text{-Pb}^{2+}$; (2) as reported earlier (see ref 17b), the disproportionation of $\text{Q}^{\cdot-}$ into Q^{2-} and Q in the presence of metal ion may take place. Thus, $2 \times \text{TTF}^{\cdot+}\text{-Q}^{\cdot-}\text{-Pb}^{2+} \rightarrow \text{TTF}^{\cdot+}\text{-Q}^{2-}\text{-Pb}^{2+} + \text{TTF}^{\cdot+}\text{-Q} + \text{Pb}^{2+}$; (3) the overall reaction can be represented as $2 \times \text{TTF}^{\cdot+}\text{-Q} + \text{Pb}^{2+} \rightarrow \text{TTF}^{\cdot+}\text{-Q}^{2-}\text{-Pb}^{2+} + \text{TTF}^{\cdot+}\text{-Q}$.

(17) (a) Giffard, M.; Mabon, G.; Leclair, E.; Mercier, N.; Allain, M.; Gorgues, A.; Molinie, P.; Neilands, O.; Krief, P.; Khodorkovsky, V. *J. Am. Chem. Soc.* **2001**, *123*, 3852–3853. (b) Fukuzumi, S.; Nishizawa, N.; Tanaka, T. *J. Chem. Soc., Perkin Trans. 2* **1985**, 371–378. (c) Fukuzumi, S.; Hironaka, K.; Nishizawa, N.; Tanaka, T. *Bull. Chem. Soc. Jpn.* **1983**, *56*, 2220–2227.

(18) The use of molecular and/or ion recognition to promote ICT (rather than intramolecular electron transfer) was reported previously: (a) Witulski, B.; Weber, M.; Bergstrasser, U.; Desvergne, J.-P.; Bassani, D. M.; Bouas-Laurent, H. *Org. Lett.* **2001**, *3*, 1467–1470. (b) McClenaghan, N. D.; Grote, Z.; Darriet, K.; Zimine, M.; Williams, R. M.; De Cola, L.; Bassani, D. M. *Org. Lett.* **2005**, *7*, 807–810.

(19) On the basis of the absorbance variation at 845 nm vs the amount of Sc^{3+} , the reaction stoichiometry between dyad **1** (abbreviated as TTF–Q) and Sc^{3+} was estimated to be 2:1 (see ref 16). In the case of Zn^{2+} , the absorbance at 845 nm was rather weak and moreover it was found that the absorbance also varied with the reaction time. Thus, it was difficult to estimate the corresponding stoichiometry.

(20) In the case of Sc^{3+} , an additional ESR signal was detected in the diluted solution, which may be ascribed to the radical anion– Sc^{3+} complex (see Figure S1 of the Supporting Information). This may be understandable since the disproportionation equilibrium among $\text{Q}^{\cdot-}$, Q^{2-} , and Q in the presence of metal ions is dependent on the Lewis acidity of the metal ion (see ref 24e).

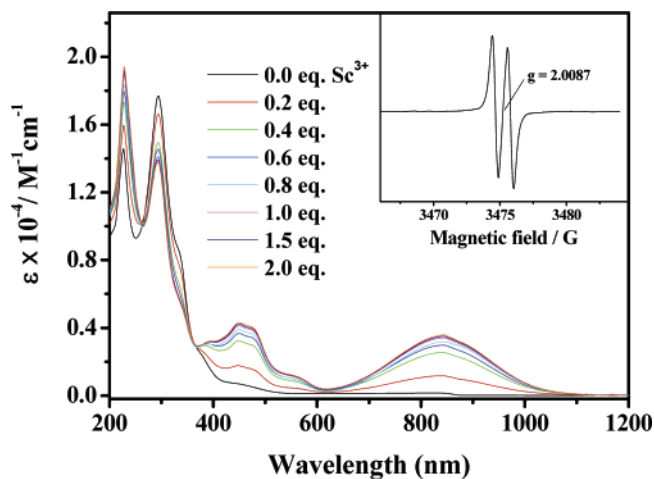


Figure 3. Absorption spectra (with an ϵ scale) of dyad **1** recorded in a mixture of CH_2Cl_2 and CH_3CN (1:1, v/v; 5.0×10^{-5} M) in the presence of increasing amounts of Sc^{3+} [$\text{Sc}(\text{SO}_3\text{CF}_3)_3$]; inset shows the ESR spectrum of dyad **1** (1.0×10^{-4} M) in $\text{CH}_2\text{Cl}_2/\text{CH}_3\text{CN}$ (1:1, v/v) in the presence of Sc^{3+} (1.0×10^{-4} M) recorded at room temperature.

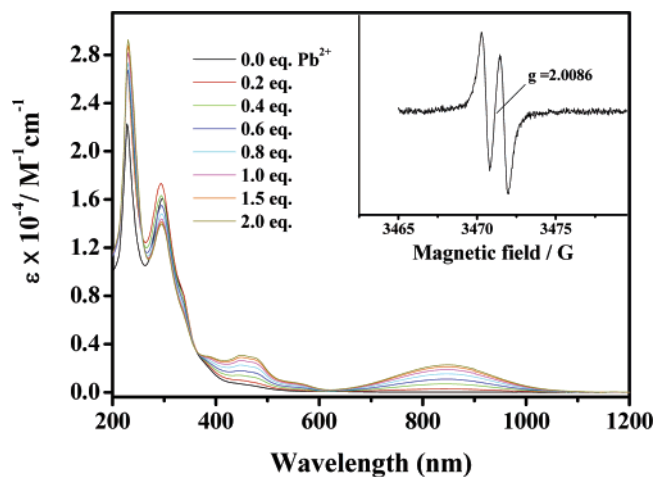


Figure 5. Absorption spectra (with an ϵ scale) of dyad **2** recorded in a mixture of CH_2Cl_2 and CH_3CN (1:1, v/v; 5.0×10^{-5} M) in the presence of increasing amounts of Pb^{2+} [$\text{Pb}(\text{ClO}_4)_2$]; inset shows the ESR spectrum of dyad **2** (1.0×10^{-4} M) in $\text{CH}_2\text{Cl}_2/\text{CH}_3\text{CN}$ (1:1, v/v) in the presence of Pb^{2+} (1.0×10^{-4} M) recorded at room temperature.

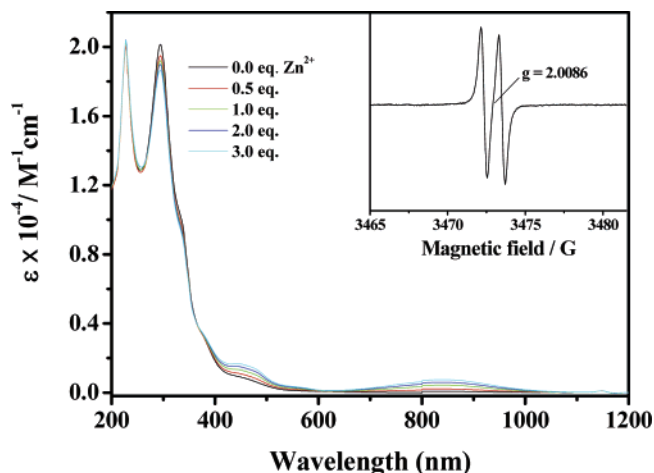


Figure 4. Absorption spectra (with an ϵ scale) of dyad **1** recorded in a mixture of CH_2Cl_2 and CH_3CN (1:1, v/v; 5.0×10^{-5} M) in the presence of increasing amounts of Zn^{2+} [$\text{Zn}(\text{ClO}_4)_2$]; inset shows the ESR spectrum of dyad **1** (1.0×10^{-4} M) in $\text{CH}_2\text{Cl}_2/\text{CH}_3\text{CN}$ (1:1, v/v) in the presence of Zn^{2+} (1.0×10^{-4} M) recorded at room temperature.

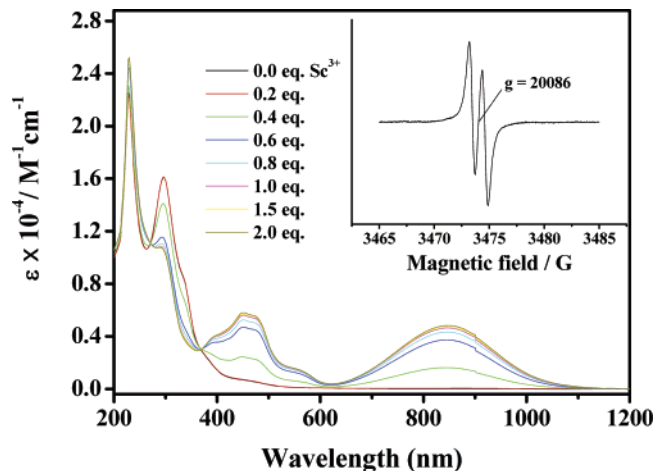


Figure 6. Absorption spectra (with an ϵ scale) of dyad **2** recorded in a mixture of CH_2Cl_2 and CH_3CN (1:1, v/v; 5.0×10^{-5} M) in the presence of increasing amounts of Sc^{3+} [$\text{Sc}(\text{SO}_3\text{CF}_3)_3$]; inset shows the ESR spectrum of dyad **2** (1.0×10^{-4} M) in $\text{CH}_2\text{Cl}_2/\text{CH}_3\text{CN}$ (1:1, v/v) in the presence of Sc^{3+} (1.0×10^{-4} M) recorded at room temperature.

Efficient intramolecular electron transfer was even observed for dyad **2** (Scheme 1) with an even longer spacer (containing oligoethylene glycol chain) as indicated by the absorption spectra of dyad **2** in the presence of metal ions. As shown in Figure 5, where the absorption spectra of dyad **2** in the presence of Pb^{2+} is displayed, absorption bands at 450 and 845 nm are observed, indicating the formation of the radical cation of the TTF unit.²² Their intensities were weaker than those of dyad **1** (see Figure 1) but still 6 times higher than those of dyad **3** (see Figure 7). Strong ESR signals with two peaks were also detected for dyad **2** in the presence of Pb^{2+} as shown in the inset of Figure 5. Similar absorption and ESR spectra were also detected for dyad **2** in the presence of Sc^{3+} and Zn^{2+} (see Figure 6 and Figure S4

of the Supporting Information).²² These results clearly showed that intramolecular electron transfer can also occur within dyad **2** with a much longer spacer in the presence of metal ion (Sc^{3+} , Pb^{2+} , Zn^{2+}).

The absorption spectra of dyad **3** in which the TTF and quinone units are linked by an alkyl chain were recorded in the presence of metal ions under the same conditions as those for dyad **1**. Figure 7 shows the absorption spectra of dyad **3** in the presence of different amounts of Pb^{2+} . Although the absorption bands at 450 and 845 nm were observed, their intensities were rather weaker than those of dyad **1** in the presence of Pb^{2+} . Only rather weak ESR signals were detected for the solution of dyad **3** containing 1.0 equiv of Pb^{2+} . Such comparative results implied that the oligoethylene glycol chain in dyad **1** (besides the radical anion of quinone) may also coordinate with metal ions (e.g., Pb^{2+}) as to be discussed below.

2.3. Electrochemical Studies. In order to understand the electron-transfer mechanism within dyads **1** and **2**, electrochemical studies were carried out. The redox potentials of dyads **1** and **2** were determined: $E^{1/2}(\text{ox}_1) = 0.55$ V, $E^{1/2}(\text{ox}_2) = 0.87$

(21) For dyad **1** in the presence of 1 equiv of Sc^{3+} , the absorbance at 845 nm was 0.18 ($\epsilon = 3600$) and the ESR signal intensity (integration area) was 49 840; for dyad **1** in the presence of 1 equiv of Pb^{2+} , they were 0.14 ($\epsilon = 2800$) and 19 780; for dyad **1** in the presence of 1 equiv of Zn^{2+} , they were 0.03 ($\epsilon = 600$) and 9210.

(22) On the basis of the absorbance variation at 845 nm vs the amount of Pb^{2+} or Sc^{3+} (see Figures 5 and 6), the reaction stoichiometry between dyad **2** (abbreviated as TTF-Q) and Pb^{2+} or Sc^{3+} was estimated to be ca. 2:1 (see ref 16).

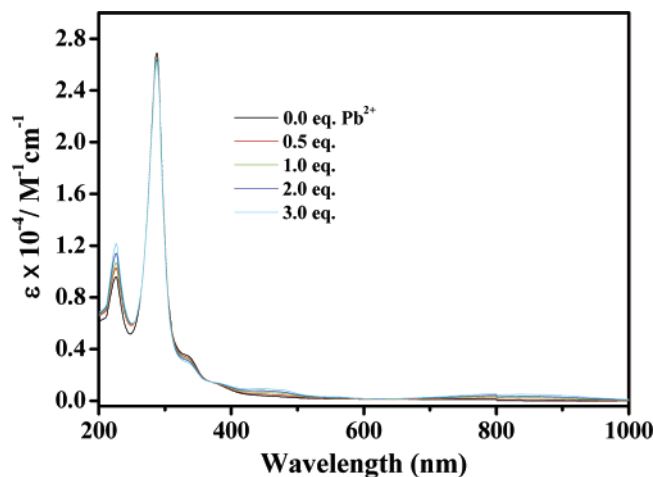


Figure 7. Absorption spectra (with an ϵ scale) of dyad **3** recorded in a mixture of CH_2Cl_2 and CH_3CN (1:1, v/v; 5.0×10^{-5} M) in the presence of increasing amounts of Pb^{2+} [$\text{Pb}(\text{ClO}_4)_2$].

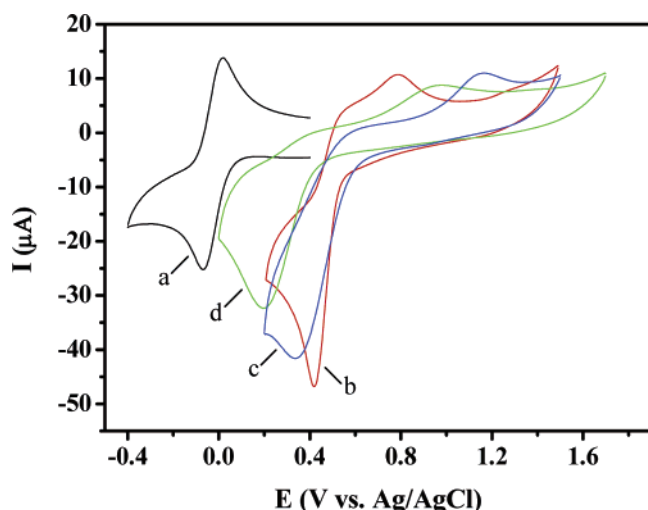


Figure 8. Cyclic voltammograms of compound **5** (2.0×10^{-3} M) before (a, black) and after addition of 4.0 equiv of $\text{Pb}(\text{ClO}_4)_2$ (b, red), $\text{Sc}(\text{SO}_3\text{CF}_3)_3$ (c, blue), and $\text{Zn}(\text{ClO}_4)_2$ (d, green) in $\text{CH}_2\text{Cl}_2/\text{CH}_3\text{CN}$ (1:1, v/v) at a scan rate of 100 mV s^{-1} .

V, and $E^{1/2}(\text{red}) = -0.05 \text{ V}$ for dyad **1**; $E^{1/2}(\text{ox}_1) = 0.54 \text{ V}$, $E^{1/2}(\text{ox}_2) = 0.86 \text{ V}$, and $E^{1/2}(\text{red}) = -0.04 \text{ V}$ for dyad **2**.²³ For comparison, redox potentials of reference compounds **4** and **5** were also measured: $E^{1/2}(\text{ox}_1) = 0.54 \text{ V}$, $E^{1/2}(\text{ox}_2) = 0.86 \text{ V}$ for **4**; $E^{1/2}(\text{red}_1) = -0.05 \text{ V}$ (corresponding to $\text{Q}/\text{Q}^{\bullet-}$ redox couple); $E^{1/2}(\text{red}_2) = -0.76 \text{ V}$ (corresponding to $\text{Q}^{\bullet-}/\text{Q}^{2-}$ redox couple) for **5**. These results can lead to the following conclusions: (1) the electron donor–acceptor interaction within dyads **1** and **2** can be neglected in their ground states. This agrees well with the absorption spectral studies as discussed above; (2) the electron transfer between the TTF and quinone units of dyads **1** and **2** is not thermodynamically feasible.

Figure 8 shows the cyclic voltammograms of compound **5** in the presence of metal ions (Pb^{2+} , Sc^{3+} , Zn^{2+}) at a scan rate of 100 mV s^{-1} . The original redox wave around -0.05 V (corresponding to the $\text{Q}/\text{Q}^{\bullet-}$ redox couple) disappeared, and an irreversible redox wave was detected in the presence of each

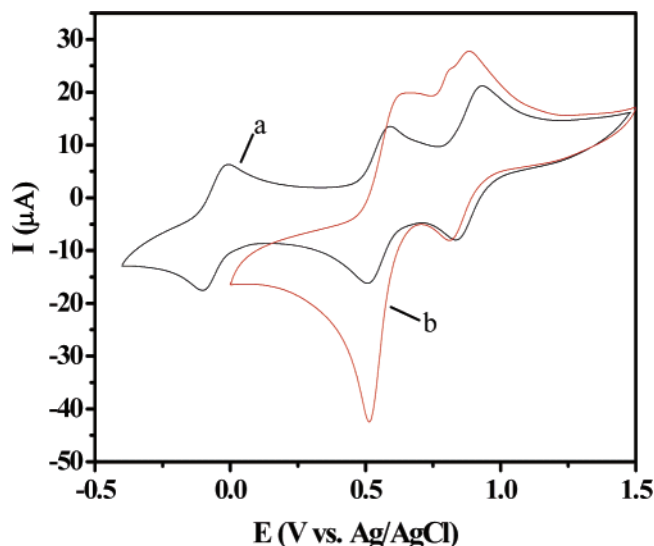


Figure 9. Cyclic voltammograms of dyad **1** (1.0×10^{-3} M) (a, black) before and (b, red) after addition of 2.0 equiv of $\text{Pb}(\text{ClO}_4)_2$ in $\text{CH}_2\text{Cl}_2/\text{CH}_3\text{CN}$ (1:1, v/v) at a scan rate of 100 mV s^{-1} .

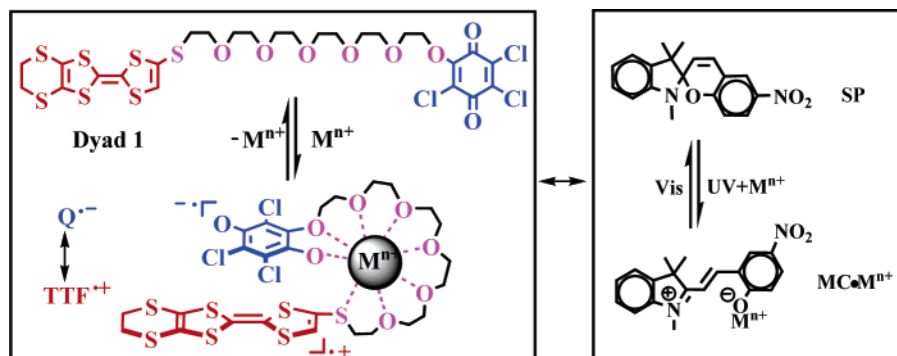
metal ion. Moreover, the new irreversible cathodic waves upon addition of metal ions (Pb^{2+} , Sc^{3+} , Zn^{2+}) were found to be dependent on the sweep rates (see Figures S8–S10 of the Supporting Information). This was due to the fact that the disproportionation of the radical anion of quinone ($\text{Q}^{\bullet-}$) into the corresponding Q^{2-} and neutral Q in the presence of metal ion was fast on the time-scale of cyclic voltammetric measurement.^{17b} On the basis of the method reported by Fukuzumi and co-workers,^{17b,c} the reduction potential (E_{red}°) of **5** was estimated to be 0.33, 0.45, and 0.28 V in the presence of Pb^{2+} (4.0 equiv), Sc^{3+} (4.0 equiv), and Zn^{2+} (4.0 equiv), respectively (Figures S11–S13 of the Supporting Information). These results clearly showed that the reduction potential of the reference compound **5** was significantly shifted to the positive region after addition of metal ions (Pb^{2+} , Sc^{3+} , Zn^{2+}). Under the same conditions, the variation of the oxidation potentials of reference compound **4** was negligible.

The cyclic voltammograms of dyads **1** and **2** were also measured in the presence of metal ion (Pb^{2+} , Sc^{3+} , Zn^{2+}) (see Figures S6 and S7 of the Supporting Information). As an example, Figure 9 shows the cyclic voltammogram of dyad **1** in the presence of Pb^{2+} together with that of dyad **1** in the absence of Pb^{2+} . Clearly, the original reduction wave (corresponding to $\text{Q}/\text{Q}^{\bullet-}$ redox couple) of the quinone unit was absent after addition of Pb^{2+} , and two redox waves in the range of 0.5–1.0 V were detected. For the first redox wave, the cathodic peak current was found to be much larger than the corresponding anodic peak current. As discussed for compound **5**, the redox wave due to the quinone unit of dyad **1** would be shifted to positive range and became irreversible. Therefore, it is probable that the redox wave due to the quinone unit became overlapped with those of the TTF unit upon addition of metal ions. The second oxidation and reduction peaks should be related to the redox reaction between the radical cation ($\text{TTF}^{\bullet+}$) and dication (TTF^{2+}) of the TTF unit.

On the basis of the reduction potentials of **5** in the presence of metal ion (Pb^{2+} , Sc^{3+} , Zn^{2+}) and the oxidation potential of **4**, it can be concluded that the electron transfer between the TTF and quinone units of dyads **1** and **2** would become

(23) Additional irreversible redox waves in the range of -0.78 to -0.92 V and -0.84 to -0.91 V were detected for dyads **1** and **2**, respectively (see Figure S5 of the Supporting Information). All redox potentials were represented by reference to Ag/AgCl .

Scheme 2. Proposed Mechanism for the Metal Ion-Promoted Intramolecular Electron Transfer and the Photomodulation in the Presence of Spiropyran



thermodynamically more feasible in the presence of these metal ions. But, the electron-transfer processes within dyads **1** and **2** are still endothermic by just considering the redox potentials of the TTF and quinone units in the presence of metal ion (Pb^{2+} , Sc^{3+} , Zn^{2+}). As to be discussed below, other forces come into play by stabilizing the charge-separated transitional state, therefore making the electron-transfer process exothermic.

According to the previous results reported by Fukuzumi and co-workers,^{24,25} the variation of the reduction potentials of **5** in the presence of $\text{Pb}^{2+}/\text{Sc}^{3+}/\text{Zn}^{2+}$ is due to the coordination of the radical anion of quinone ($\text{Q}^{\bullet-}$) with metal ions. Therefore, we propose that the intramolecular electron transfer within dyad **1** in the presence of metal ions is promoted by the coordination of the radical anion of the quinone ($\text{Q}^{\bullet-}$) unit with metal ions.²⁶ At least, this proposition is supported by the following finding: addition of thiourea to the solution of dyad **1** containing Pb^{2+} leads to the disappearance of the absorption bands at 450 and 845 nm. This is likely due to the stronger binding of thiourea with Pb^{2+} than the radical anion of quinone.

Moreover, the comparative studies of dyad **3** with dyads **1** and **2** as discussed above indicate that the oligoethylene glycol chain in dyad **1**, besides the radical anion of quinone ($\text{Q}^{\bullet-}$), may also coordinate with metal ions (e.g., Pb^{2+}). The synergic coordination of the oligoethylene glycol chain and the radical anion of quinone with metal ion could further stabilize the corresponding charge-separation state by enhancing the intramolecular electronic attraction between the radical cation of TTF and the radical anion of quinone ($\text{Q}^{\bullet-}$)²⁶ as illustrated in Scheme 2, thus further facilitating the electron-transfer processes within dyads **1** and **2**. It is known that Sc^{3+} shows a preference for oxygen coordination. Apart from the oxygen atoms of the oligoethylene glycol chain, the sulfur atoms of the TTF unit (see Scheme 2) may be also involved in the coordination with metal ions, in particular for Pb^{2+} , which is a very poor

oxidophile, preferring the much softer sulfur ligands. This may also explain the fact that Pb^{2+} can facilitate the electron-transfer processes within dyads **1** and **2** more efficiently than Zn^{2+} . In fact, a similar mechanism was proposed for the metal ion-promoted intramolecular π - π interactions.²⁷

2.4. Photomodulation of the Electron Transfer. On the basis of the synergic coordination model (Scheme 2), it was anticipated that it was possible to modulate the thermal electron-transfer processes within dyads **1** and **2** through competitive binding of metal ions by other ligands. The competitive binding of metal ions by additional ligands would shift the disproportionation equilibrium among $\text{Q}^{\bullet-}$, Q^{2-} , and Q (quinone unit) in the presence of metal ion (see refs 16 and 17b), and thus the back electron transfer from $\text{Q}^{\bullet-}$ to $\text{TTF}^{\bullet+}$ (radical cation of the TTF unit) would occur accordingly. As described earlier, the open form (MC) of SP can coordinate with metal ions ($\text{MC}\cdot\text{M}^{n+}$), while SP does not show this property; moreover, metal ion can be released from $\text{MC}\cdot\text{M}^{n+}$ after visible light irradiation, and concomitantly MC is transformed into SP.^{28,29} Therefore, it would be interesting to study the intramolecular electron-transfer processes within dyads **1** and **2** in the presence of metal ions and SP under UV and visible light irradiation.

Because the reversible transformation among SP, MC, and $\text{MC}\cdot\text{M}^{n+}$ can be easily carried out in THF, the mixture of $\text{CH}_2\text{-Cl}_2$ and THF (v/v, 1:1) was employed for absorption spectral measurements. As an example, Figure 10 shows the variation of the absorption spectra of dyad **1** containing Pb^{2+} (1.0 equiv) in the presence of SP (6.0 equiv) under UV and visible light irradiation. After UV light irradiation for 100 s, the absorption intensity at 845 nm was reduced to 27% of that of the initial value. But, the absorption band at 845 nm as well as that at 450 nm still existed even after UV light irradiation for 300 s.

- (24) (a) Fukuzumi, S.; Yoshida, Y.; Okamoto, K.; Imahori, H.; Araki, Y.; Ito, O. *J. Am. Chem. Soc.* **2002**, *124*, 6794–6795. (b) Fukuzumi, S.; Okamoto, K.; Imahori, H. *Angew. Chem., Int. Ed.* **2002**, *41*, 620–622. (c) Fukuzumi, S.; Okamoto, K.; Yoshida, Y.; Imahori, H.; Araki, Y.; Ito, O. *J. Am. Chem. Soc.* **2003**, *125*, 1007–1013. (d) Okamoto, K.; Imahori, H.; Fukuzumi, S. *J. Am. Chem. Soc.* **2003**, *125*, 7014–7021. (e) Fukuzumi, S.; Ohkubo, K.; Okamoto, T. *J. Am. Chem. Soc.* **2002**, *124*, 14147–14155.
- (25) (a) Fukuzumi, S.; Mori, H.; Imahori, H.; Suenobu, T.; Araki, Y.; Ito, O.; Kadish, K. M. *J. Am. Chem. Soc.* **2001**, *123*, 12458–12465. (b) Yuasa, J.; Suenobu, T.; Fukuzumi, S. *J. Am. Chem. Soc.* **2003**, *125*, 12090–12091. (c) Fukuzumi, S. *Org. Biomol. Chem.* **2003**, *1*, 609–620. (d) Yuasa, J.; Suenobu, T.; Fukuzumi, S. *Chem. Phys. Chem.* **2006**, *7*, 942–954.
- (26) The disproportionation reaction of $\text{Q}^{\bullet-}$ into the corresponding Q^{2-} and neutral Q unit may occur easily in the presence of metal ions at room temperature (see refs 16 and 17b). This is in agreement with the fact that no ESR signals due to the $\text{Q}^{\bullet-}$ were detected for the solutions of dyads **1** and **2** after addition of metal ions at room temperature.

- (27) (a) Ajayaghosh, A.; Arunkumar, E.; Daub, J. *Angew. Chem., Int. Ed.* **2002**, *41*, 1766–1769. (b) Arunkumar, E.; Chithra, P.; Ajayaghosh, A. *J. Am. Chem. Soc.* **2004**, *126*, 6590–6598. (c) Arunkumar, E.; Ajayaghosh, A.; Daub, J. *J. Am. Chem. Soc.* **2005**, *127*, 3156–3164.
- (28) (a) Wojtyk, J. T. C.; Kazmaier, P. M.; Buncel, E. *Chem. Commun.* **1998**, 1703–1704. (b) Winkler, J. D.; Bowen, C. M.; Michelet, V. *J. Am. Chem. Soc.* **1998**, *120*, 3237–3242. (c) Wojtyk, J. T. C.; Wasey, A.; Kazmaier, P. M.; Hoz, S.; Buncel, E. *J. Phys. Chem. A* **2000**, *104*, 9046–9055. (d) Wojtyk, J. T. C.; Kazmaier, P. M.; Buncel, E. *Chem. Mater.* **2001**, *13*, 2547–2551. (e) Suzuki, T.; Kawata, Y.; Kahata, S.; Kato, T. *Chem. Commun.* **2003**, 2004–2005. (f) Suzuki, T.; Kato, T.; Shinozaki, H. *Chem. Commun.* **2004**, 2036–2037. (g) Wang, G.; Bohaty, A. K.; Zharov, I.; White, H. S. *J. Am. Chem. Soc.* **2006**, *128*, 13553–13558.
- (29) (a) Guo, X.; Zhang, D.; Wang, T.; Zhu, D. *Chem. Commun.* **2003**, 914–915. (b) Guo, X.; Zhang, D.; Tao, H.; Zhu, D. *Org. Lett.* **2004**, *6*, 2491–2494. (c) Guo, X.; Zhang, D.; Zhu, D. *J. Phys. Chem. B* **2004**, *108*, 212–217. (d) Guo, X.; Zhang, D.; Zhu, D. *Adv. Mater.* **2004**, *16*, 125–130. (e) Wen, G.; Yan, J.; Zhou, Y.; Zhang, D.; Mao, L.; Zhu, D. *Chem. Commun.* **2006**, 3016–3018.

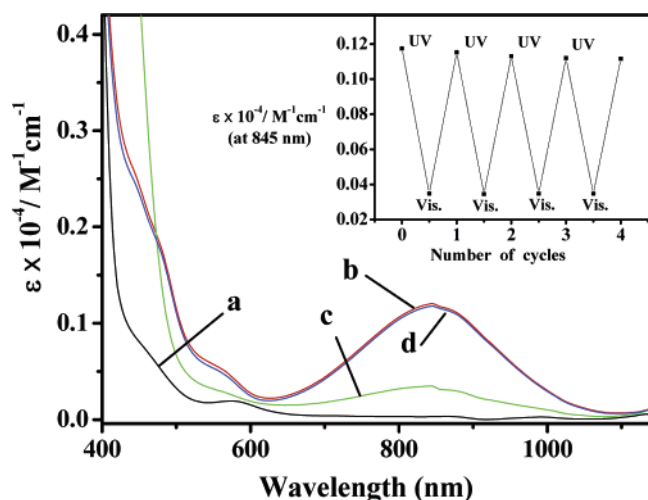


Figure 10. Absorption spectra (with an ϵ scale) of the mixture of dyad **1** (5.0×10^{-5} M) and SP (3.0×10^{-4} M) (a, black) before and (b, red) after addition of $\text{Pb}(\text{ClO}_4)_2$ (5.0×10^{-5} M), (c, green) after UV light (365 nm) irradiation for 100 s, and (d, blue) after further visible light irradiation for 100 s; inset shows the variation of ϵ at 845 nm.

This is likely due to the fact that the binding constant of MC with Pb^{2+} is not so large that Pb^{2+} in the solution could not be fully coordinated by MC. Interestingly, visible light irradiation of the above solution that had been treated by UV light irradiation led to the restoration of the absorption intensity at 845 nm (also that at 450 nm). This is obviously due to the release of Pb^{2+} from $\text{MC}\cdot\text{Pb}^{2+}$ after visible light irradiation. In fact, up to four cycles of such increase–decrease for the absorption intensity at 845 nm, by applying UV light and visible light alternatively, can be realized (see the inset of Figure 10) for the solution of dyad **1** containing Pb^{2+} in the presence of SP.

Moreover, the ESR signal intensity of the solution of dyad **1** containing Pb^{2+} and SP can be tuned by alternating UV and visible light irradiation; the ESR signal intensity became rather weak after UV light irradiation, and it can be almost recovered after further visible light irradiation (see Figure S3 of the Supporting Information). On the basis of these absorption and ESR spectral studies, it may be concluded that the intramolecular electron-transfer process within dyad **1** facilitated by Pb^{2+} can be reversibly modulated by UV–vis light irradiation in the presence of SP.

Similarly, the Pb^{2+} -promoted electron transfer between the TTF and quinone units of dyad **2** can also be modulated by UV and visible light irradiation in the presence of SP. The complex $\text{MC}\cdot\text{Sc}^{3+}$ was found to be rather stable, and thus Sc^{3+} could be only partially released from $\text{MC}\cdot\text{Sc}^{3+}$ after visible light irradiation. Therefore, the Sc^{3+} -promoted electron transfer with dyads **1** and **2** cannot be reversibly tuned by UV–vis light irradiation in the presence of SP.³⁰

3. Conclusion

In summary, we reported for the first time the intramolecular electron transfer within a substituted TTF–quinone dyad **1** (and dyad **2**) in the presence of metal ions (Sc^{3+} , Pb^{2+} , Zn^{2+}). On the basis of the electrochemical studies of reference compound

5 and the comparative studies with dyad **3**, it was proposed that the synergic coordination of the radical anion of quinone²⁶ and the oligoethylene glycol chain with metal ions should be responsible for stabilizing the charge-separation state and thus facilitating the electron-transfer process. But, the proposed structure of the coordination complex needs to be investigated further. Most interestingly, it was demonstrated that it was possible to modulate the intramolecular electron-transfer process within dyad **1** by employing the unique features of SP.

4. Experimental Section

Chemicals. The following chemical reagents were purchased from the indicated suppliers and used without purification: $\text{CsOH}\cdot\text{H}_2\text{O}$ (Acros), tetra-*n*-butylammonium hexafluorophosphate (Acros), 2-bromoethanol (Acros), hexaethylene glycol (Fluka), tetrachloro-1,4-benzoquinone (Acros), succinic anhydride (Acros), 4-(dimethylamino)pyridin (Merck), *N,N'*-dicyclohexyl-carbodiimide (Acros), lead perchlorate (Acros), and scandium triflate (Aldrich). CH_2Cl_2 and CH_3CN were distilled from CaH_2 , and THF was distilled from sodium/benzophenone prior to use. All other chemicals were local products of analytical grade. Deionized and distilled water was used throughout.

Characterization Techniques. ^1H NMR spectra and ^{13}C NMR were recorded on a Bruker 400 MHz instrument. Mass spectra (MS) were recorded with AEI-MS50 and BEFLEX III spectrometer. ESR spectra were obtained by a Bruker-E500 spectrometer. Absorption spectra were measured with JASCO V-570 UV–vis spectrophotometer in a 1 cm quartz cell. Cyclic voltammetric measurements were performed on a CHI 660B system in a standard three-electrode cell, with Pt as the working and counter electrodes and Ag/AgCl electrode (saturated KCl) as the reference electrode which was connected to the electrochemical cell through a Luggin capillary. The scan rate was 100 mV/s, and *n*- $\text{Bu}_4\text{-NPF}_6$ (0.1 M) was used as supporting electrolyte. The light irradiation experiments were carried out by putting the solutions ca. 10 cm below the light sources; a 100 W UV lamp (365 nm) and 150 W tungsten lamp were used as UV and visible light sources, respectively.

Compound 4. To a solution of **6** (0.68 g, 1.8 mmol) in anhydrous degassed THF was added a solution of $\text{CsOH}\cdot\text{H}_2\text{O}$ (0.36 g, 2.1 mmol) in anhydrous degassed MeOH over a period of 10 min. The mixture was stirred for an additional 30 min. A solution of hexaethyleneglycol–monotoluenesulfonate (1.57 g, 3.6 mmol) in anhydrous degassed THF was added. The solution was stirred overnight. After separation by column chromatography (silica gel) using ethylacetate as eluant, compound **4** (0.88 g) was obtained as a yellow oil in 83% yield. ^1H NMR (400 MHz, CDCl_3): δ 6.44 (1H, s), 3.72 (2H, m), 3.66–3.60 (20H, m), 3.29 (4H, s), 2.93 (2H, t, $J = 6.4$ Hz), 2.67 (1H, br). ^{13}C NMR (100 MHz, CDCl_3): δ 126.5, 122.9, 117.9, 113.9, 113.8, 106.6, 72.5, 70.6, 70.52, 70.49, 70.44, 70.3, 69.6, 61.7, 35.2, 30.2. HR-MS (EI): calcd for $\text{C}_{20}\text{H}_{30}\text{O}_6\text{S}_7$, 590.0087; found, 590.0084.

Compound 5. To a solution of hexaethylene glycol (0.29 g, 1.0 mmol) in dry THF was added petroleum ether rinsed NaH (52%, 46 mg, 1.0 mmol) in N_2 atmosphere at 0 °C. The mixture was stirred for 20 min. Tetrachloro-1,4-benzoquinone (0.49 g, 2.0 mmol) was added, after which the mixture was allowed to attain room temperature. After being stirred for 1 h the reaction mixture was filtered. The filtrate was concentrated in vacuo. The residue was purified by column chromatography on silica gel using ethylacetate as eluant; **5** was obtained as a yellow oil (0.14 g) in 26% yield. ^1H NMR (400 MHz, CDCl_3): δ 4.66 (2H, t, $J = 5.4$ Hz), 3.74 (2H, t, $J = 5.5$ Hz), 3.69–3.53 (20H, m), 2.88 (1H, br). ^{13}C NMR (100 MHz, CDCl_3): δ 172.4, 171.6, 155.1, 139.9, 138.4, 125.2, 73.2, 72.3, 70.5, 70.4, 70.3, 70.2, 70.0, 61.3. MS (MALDI-TOF): m/z 512.9 [$\text{M} + \text{Na}$] $^+$. HR-MS: calcd for $\text{C}_{18}\text{H}_{25}\text{-Cl}_3\text{O}_6 + \text{H}^+$, 491.0642; found, 491.0648.

Compound 7. A solution of **4** (0.59 g, 1.0 mmol), succinic anhydride (0.2 g, 2.0 mmol), K_2CO_3 (0.69 g, 5.0 mmol) in dry DMF (25 mL) was stirred for 24 h at ambient temperature. A volume of 20 mL of

(30) Because the intensities of absorption bands at 845 and 450 nm were weak for dyads **1** and **2** in the presence of Zn^{2+} in $\text{CH}_2\text{Cl}_2/\text{THF}$ (v/v, 1:1), the corresponding photomodulation experiments were not performed.

HCl (1 N) was added carefully under vigorous stirring at 0 °C. The mixture was extracted with CH₂Cl₂ (3 × 50 mL). The combined organic phases were washed with water (5 × 50 mL), dried (MgSO₄), and concentrated under reduced pressure to give **7** (0.66 g) as a red oil in 96% yield. ¹H NMR (400 MHz, CDCl₃): δ 9.65–8.10 (1H, br), 6.44 (1H, s), 4.26 (2H, t, *J* = 5.9 Hz), 3.66–3.59 (20H, m), 3.28 (4H, s), 2.92 (2H, t, *J* = 6.3 Hz), 2.64 (4H, s). ¹³C NMR (100 MHz, CDCl₃): δ 175.8, 171.9, 126.3, 122.8, 117.7, 113.7, 113.6, 106.4, 70.39, 70.38, 70.30, 70.26, 69.4, 68.8, 63.7, 35.0, 30.0, 28.9, 28.8. MS (MALDI-TOF): *m/z* 690.1 [M + H]⁺.

Dyad 1. To a solution of **4** (0.59 g, 1.0 mmol) in dry THF was added petroleum ether rinsed NaH (52%, 0.23 g, 5.0 mmol) in N₂ atmosphere at room temperature. The mixture was stirred for 20 min, whereupon tetrachloro-1,4-benzoquinone (0.49 g, 2.0 mmol) was added. After being stirred overnight the reaction mixture was filtered. The filtrate was concentrated in vacuo. After column chromatography (CH₂-Cl₂/EtOAc, 4:1) on silica gel, **1** was obtained as a yellow oil (0.35 g) in 44% yield. FT-IR (KBr, cm⁻¹): 1682 (C=O). ¹H NMR (400 MHz, CDCl₃): δ 6.44 (1H, s), 4.69 (2H, t, *J* = 4.4 Hz), 3.78 (2H, t, *J* = 4.4 Hz), 3.66–3.30 (18H, m), 3.29 (4H, s), 2.94 (2H, t, *J* = 6.0 Hz). ¹³C NMR (100 MHz, CDCl₃): δ 172.6, 171.8, 155.3, 140.1, 138.7, 126.5, 125.5, 122.9, 117.9, 113.8, 106.6, 73.5, 70.7, 70.6, 70.5, 70.4, 70.3, 69.6, 35.3, 30.1. HR-MS (EI): calcd for C₂₆H₂₉Cl₃O₈S₇, 797.8973, 799.8944; found, 797.8960, 799.8953.

Dyad 2. A solution of **5** (0.49 g, 1.0 mmol), **7** (0.69 g, 1.0 mmol), and DMAP (12 mg, 0.1 mmol) in 30 mL of dry CH₂Cl₂ was stirred at 0 °C for 10 min. A solution of DCC (0.25 g, 1.2 mmol) in 10 mL of dry CH₂Cl₂ was added dropwise under N₂ atmosphere. After addition the temperature was allowed to reach room temperature, and the mixture was stirred overnight. The white urea precipitate was removed by filtration. Evaporation of the solvent afforded a crude material that was purified by column chromatography (ethyl acetate/methanol, 50:1); **2** was obtained as a yellow oil (0.35 g, 0.3 mmol) in 30% yield. ¹H NMR (400 MHz, CDCl₃): δ 6.43 (1H, s), 4.69 (2H, t, *J* = 5.4 Hz), 4.23 (4H, m), 3.67 (2H, t, *J* = 5.3 Hz), 3.70–3.56 (38H, m), 3.28 (4H, s),

2.92 (2H, t, *J* = 7.5 Hz), 2.65 (4H, s). ¹³C NMR (100 MHz, CDCl₃): 172.6, 172.2, 171.8, 155.3, 151.7, 140.2, 138.7, 126.5, 125.5, 122.9, 117.9, 113.9, 113.8, 106.6, 73.4, 70.74, 70.71, 70.6, 70.5, 70.3, 69.6, 69.0, 63.8, 35.2, 30.2, 28.9. HR-MS (MALDI-TOF) calcd for C₄₂H₅₇-Cl₃O₁₇S₇ + 2H⁺, 1164.0857, 1166.0835, 1168.0814; found, 1164.0828, 1166.0805, 1168.0781.

Dyad 3. This was prepared in a similar manner as for dyad **1** from compound **8** as a gray solid in 48% yield. ¹H NMR (400 MHz, CDCl₃): δ 6.41 (1H, s), 4.66 (2H, t, *J* = 8.4 Hz), 3.29 (s, 4H), 3.08 (2H, t, *J* = 8.4 Hz). ¹³C NMR (100 MHz, DMSO-*d*₆): δ 173.3, 170.2, 155.0, 139.9, 138.9, 126.0, 123.9, 120.9, 113.8, 113.7, 106.4, 72.3, 35.5, 29.9. HR-MS (EI): calcd for C₁₆H₉Cl₃O₃S₇, 577.7662, 579.7633; found, 577.7651, 579.7639.

Acknowledgment. The present research was financially supported by the NSFC, the Chinese Academy of Sciences, and the State Key Basic Research Program (2006CB806201). D.-Q.Z. thanks the National Science Fund for Distinguished Young Scholars. The authors also thank the anonymous reviewers for the critical comments which enabled us to improve the manuscript greatly.

Supporting Information Available: ESR spectrum of the diluted solution of dyad **1** in the presence of Sc³⁺, ESR spectrum of compound **4** (TTF^{•+}) after oxidation, ESR spectra of dyad **1** in the presence of Pb²⁺ and spiropyran after UV-vis light irradiation, absorption and ESR spectra of dyads **2** in the presence of Zn²⁺, cyclic voltammograms of dyads **1** and **2** and compounds **4** and **5** and those in the presence of metal ions, energy-minimized conformation of dyad **1** by theoretical calculation, absorption spectra of dyads **1–3** with an ϵ scale and with an energy scale in wavenumbers. This material is available free of charge via the Internet at <http://pubs.acs.org>.

JA0702824